Transition Path Theory

Final project for the Multi-scale methods in soft matter physics course

Vincenzo Zimbardo

September 10, 2023

University of Trento, Physics department

Contents

1 Introduction

The dynamics on many complex systems is characterized by the occurrence of rare but significant events. Well-known examples include nucleation events during phase transitions, conformational changes in macromolecules, chemical reactions and many others. These events are rare because the system spends most of the time in metastable states, separated by some barrier (energetic and/or entropic), and only over time scales much larger that the typical time scale of the dynamics it undergoes a fast transition due to thermal (and possibly quantum) fluctuations.
This kind of behaviour makes extremely difficult, if not impossible, to approach the study of rare events with classical methods such as standard molecular dynamics (MD). What happens is that the computational power employed to perform the simulation is not enough, even in modern supercomputers, to simulate sufficiently long trajectories to actually observe even a single transition. In a plain MD simulation we would observe with large probability the system stuck in a meta-stable state for all the duration of the simulation.
The first theory aimed at studying this type of event was developed in 1935 and is known as Transition State Theory (TST). The basic idea behind TST is to divide the configuration space into two parts, leaving the reactant state on one side of a dividing surface and the product state on the other, and the theory only tells how this surface is crossed during the reaction. As a result, TST provides very little information about the mechanism of the transition. Moreover, if the mechanism of the reaction is totally unknown a priori (as it usually is for complex systems), it is difficult to choose a suitable dividing surface, or it may not even exist. Another drawback is that multiple crossing of the barrier, due to diffusive behaviour, leads to a poor estimate of the transition rate.
One of the most relevant technique that has been developed to go beyond TST is Transition Path Sampling (TPS), which allows to sample only in the ensemble of reactive trajectories. This was for sure a step forward, but it remains the problem of how to analyze and extract useful information from the reactive trajectories. Knowing the reactive trajectories is not generally sufficient to understand the mechanism of the reaction, and TPS per se does not tell how this analysis should be done.
Transition Path Theory (TPT) is a theoretical framework to describe the statistical properties of the reactive trajectories, and to analyze the transition-path ensemble. In principle, it permits also to bypass the sampling of the reactive paths done in TPS, directly analyzing the statistical properties of the transition path ensemble. The strenght of TPT is that it is an exact theory, regardless of the complexity of the reaction, thus it provides a solid theoretical framework for making approximations and developing efficient numerical algorithms. In TPT time averages are replaced with configuration-space (or more generally, with phase-space) averages defined over two stationary scalar and vector distributions: the transition path density distribution and the transition current. A central role is played by the forward committor function $q^+(x)$, which will be introduced in a subsequent section. The main theoretical aspects of TPT are summarized in section 3.

2 A very brief recap of the Langevin dynamics

2.1 Overdamped regime of the Langevin dynamics

The Langevin equation (named after Paul Langevin) is a stochastic differential equation (SDE) describing how a system evolves when subjected to a combination of deterministic and fluctuating ("random") forces. The dependent variables in a Langevin equation typically are collective (macroscopic) variables changing only slowly in comparison to the other (microscopic) variables of the system. The fast (microscopic) variables are responsible for the stochastic nature of the Langevin equation [1]. One application is to Brownian motion, which models the fluctuating motion of a small particle in a fluid. It is basically a Newton's equation with an additional stochastic force proportional to $\eta(t)$, a Gaussian process with zero mean and delta correlated:

$$\langle \eta_i(t) \rangle = 0 \qquad\qquad \langle \eta_i(t)\eta_j(s) \rangle = \delta_{ij}\delta(t-s) \tag{1}$$

The proportionality constant is chosen in order to satisfy the fluctuation-dissipation theorem. The overdamped limit of the Langevin equation arises when the frictional damping term dominates over the inertial term. Since the inertial term is negligible, the particle's acceleration is essentially zero. In the overdamped regime, the Langevin equation is given by:

$$\gamma_i \dot{x_i}(t) = -\frac{\partial V(x(t))}{\partial x_i} + \sqrt{2k_B T \gamma_i}\eta_i(t) \tag{2}$$

This regime is particularly relevant in situations where the particles are very small (e.g., nanoparticles) or when the fluid viscosity is high, leading to rapid damping and minimal inertia. This simplified description is widely used in various fields, such as colloidal physics, biophysics, and polymer dynamics, to model the behavior of particles undergoing Brownian motion in highly viscous environments.

2.2 Numerical solution of the overdamped Langevin equation

The overdamped Langevin equation (2) can be rewritten in the mathematical notation of SDE as

$$dx_i = f_i(x(t))dt + g_i dW_i(t) \tag{3}$$

where

$$f_i(x(t)) = -\frac{1}{\gamma_i}\frac{\partial V}{\partial x_i} \qquad\qquad g_i = \sqrt{\frac{2k_B T}{\gamma_i}} \tag{4}$$

and dW_i is the Wiener noise. Let $x_0 = x(0)$ be the initial condition.
The simplest numerical integrator for this kind of equation is the so called Euler-Maruyama scheme, which is an extension of the Euler method for ordinary differential equations. This integration scheme discretizes the time interval $[0, T]$ into N equal subintervals of width $\Delta t = T/N$. The scheme updates the configuration x at each time step using the following iterative formula:

$$x_i^{(k+1)} = x_i^{(k)} + f_i(x^{(k)})\Delta t + g_i \Delta W_i^{(k)} \tag{5}$$

where the random increments $\Delta W_i^{(k)}$ are independent and identically distributed random variables sampled from a normal distribution of zero mean and variance Δt. One can show that the Euler-Maruyama method has a strong convergence order [2] of 0.5, i.e. when increasing or decreasing the stepsize Δt, the error of the numerical solution only scales with $\Delta t^{0.5}$ [SS21]. For more general SDE's, for which $f_i = f_i(x, t)$ and $g_i = g_i(x, t)$, this method is not feasible, as it rapidly diverges. In those cases, more sophisticated integrators are needed.

[1] See Caldeira-Leggett model.

[2] In the context of numerical solution of SDE, two kind of convergence criteria are defined: *weak convergence*, which refers to the error of the average value, and *strong convergence*, which refers to the error of any specific realization of the random process.

3 Theoretical aspects of TPT

3.1 Transition Path Theory in the overdamped regime

The two main theoretical assumptions in TPT are the markovianity of the dynamics (in configuration space in the overdamped case, in phase space in general), and ergodicity. Let $\Omega \subset \mathbb{R}^n$ be the configuration space of the system, and $x(t)$, with $-\infty < t < \infty$, be a maximal solution of the overdamped Langevin equation (2). Then ergodicity with respect to the Gibbs distribution implies that, for any observable $g(x)$:

$$\lim_{T\to\infty} \frac{1}{2T} \int_{-T}^{T} g(x(t))dt = \frac{1}{\mathcal{Z}} \int_{\Omega} g(x)e^{-\beta V(x)}dx \tag{6}$$

Where $\mathcal{Z}$ is the partition function of the system. When t spans over all $\mathbb{R}$, the ergodic trajectory $x(t)$ will be involved in the rare reaction an infinite number of times. We are only interested, however, only in that pieces of the trajectory directly involved in the reaction. These pieces form, by definition, the *transition path ensemble* (TPE), and the aim is to study the statistical properties of this ensemble, which are by ergodicity independent on the particular ergodic trajectory used to generate it. To formalize mathematically, the first step is to identify in Ω two disjoint sub-regions R and P ($R, P \subset \Omega$, $R \cap P = \emptyset$), representing the reactant and the product state respectively. The following quantities are then introduced:

$$\begin{aligned} t^+_{RP}(t) &= \inf\{t' \geq t : x(t') \in R \cup P\} \\ t^-_{RP}(t) &= \sup\{t' \leq t : x(t') \in R \cup P\} \end{aligned} \tag{7}$$

which are respectively the first time in the future during which the system will be in the reactant or in the product, and the latest time in the past during which the system was in the reactant or in the product. The TPE is the set containing all the continuous restrictions of the full ergodic trajectory in which the time t belongs to the set $\{t : x(t) \notin R \cup P, x(t^+_{RP}(t)) \in P, x(t^-_{RP}(t)) \in R\}$. The first quantity we want to obtain is the probability density function of reactive trajectories $m(x|TP) =: m_T(x)$, *i.e.* the pdf that a piece of ergodic trajectory passes through the point $x \in \Omega \setminus (R \cup P)$ conditional to it to be reactive (so that to restrict its sample space to the TPE). Exploiting ergodicity, it is such that, for any observable $g(x)$

$$\lim_{T\to\infty} \frac{\int_{-T}^{T} g(x(t))\mathbb{1}_{\Omega\setminus(R\cup P)}(x(t))\mathbb{1}_R(x(t^-_{RP}(t)))\mathbb{1}_P(x(t^+_{RP}(t)))dt}{\int_{-T}^{T} \mathbb{1}_{\Omega\setminus(R\cup P)}(x(t))\mathbb{1}_R(x(t^-_{RP}(t)))\mathbb{1}_P(x(t^+_{RP}(t)))dt} = \int_{\Omega\setminus(R\cup P)} g(x)m_T(x)dx \tag{8}$$

The aim is to find an expression for $m(x|TP)$ that avoid the need to actually sample the transition paths. To this end, consider that we already know $m(x)$, the probability to find the system at configuration $x \in \Omega \setminus (R \cup P)$, as this probability density is given by the Gibbs distribution:

$$m(x) = \frac{1}{\mathcal{Z}} e^{-\beta V(x)} \tag{9}$$

with $\mathcal{Z}$ the partition function of the system. Moreover, let $\mathbb{P}(TP|x) =: P_{\mathcal{R}}(x)$ be the probability that, conditional on x, a piece of trajectory passing through that configuration is reactive. Note that, as a function of x, $P_{\mathcal{R}}(x)$ is not a probability density, but a *probability field*, *i.e.* a function that associates to each $x \in \Omega \setminus (R \cup P)$, a probability (a real number in $[0, 1]$). This probability can be expressed in terms of the so-called committor functions, defined as follows. The *forward committor* $q^+(x)$ is the probability that a trajectory initiated at point $x \in \Omega \setminus (R \cup P)$ will reach P before touching R, while the *backward committor* $q^-(x)$ is the probability that a trajectory terminated at x comes from R rather than from P. It can be proved that (see appendix A) the committor functions satisfy the *backward Kolmogorov equation* (with different boundary conditions), that in the case of Langevin overdamped dynamics reads:

$$(\nabla^2 - \beta\nabla V \cdot \nabla)q(x) = 0 \tag{10}$$

With boundary conditions given by:

$$\begin{aligned} q^+(x)|_{\partial R} &= 0 \quad q^+(x)|_{\partial P} = 1 \\ q^-(x)|_{\partial R} &= 1 \quad q^-(x)|_{\partial P} = 0 \end{aligned} \tag{11}$$

If the dynamics is invariant under time reversal, then $q^-(x) = 1 - q^+(x)$. From now on, this is assumed to be the case and the forward committor will be denoted simply as $q(x)$. Finally, the probability $P_{\mathcal{R}}$ can be expressed as $P_{\mathcal{R}}(x) = q(x)(1 - q(x))$.
At this point, we have all what the need to find an expression for the aimed $m_T(x)$. Indeed, by applying Bayes' theorem:

$$m_T(x) = \frac{1}{\mathcal{Z}_T} m(x)q(x)(1 - q(x)) \tag{12}$$

where:

$$\mathcal{Z}_T = \mathbb{P}(TP) = \int_{\Omega\setminus(R\cup P)} m(x)q(x)(1 - q(x))dx \tag{13}$$

By ergodicity, $\mathbb{P}(TP)$ is the fraction of time spent in the TPE over the total time in a long ergodic trajectory:

$$\mathcal{Z}_T = \mathbb{P}(TP) = \lim_{T\to\infty} \frac{1}{2T} \int_{-T}^{T} \mathbb{1}_{\Omega\setminus(R\cup P)}(x(t))\mathbb{1}_R(x(t^-_{RP}(t)))\mathbb{1}_P(x(t^+_{RP}(t)))dt \tag{14}$$

The transition path density $m_T(x)$ gives some interesting information about the mechanism of the reaction. For example, it allows to determine the proportion of time that the trajectory spends in any region $C \subseteq \Omega \setminus (R \cup P)$ while it is reactive, simply by integrating it over the domain C.
The knowledge of the transition path density is however not enough to fully understand the mechanism of the reaction. Consider the following scenario:

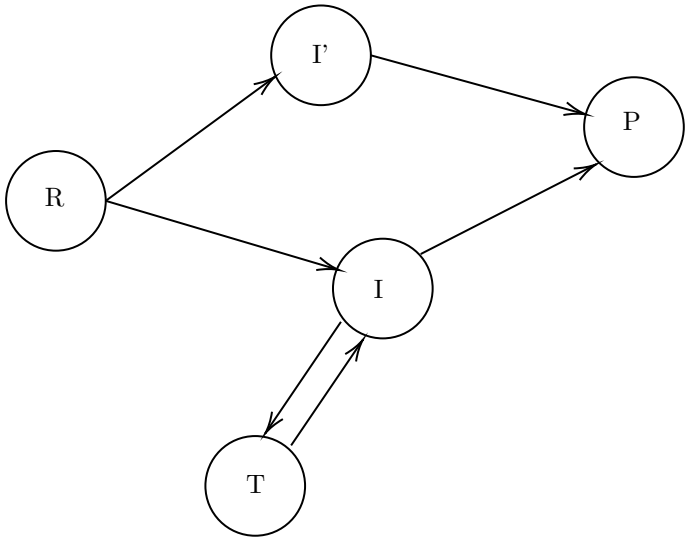

In the graph, R and P represent the reactant and the product states respectively, I and I' two intermediate metastable states (to take into account the possibility to have more than a single reaction channel), and T a trap state, *i.e.* an intermediate metastable state from which it is not possible to directly reach the product. The transition path density $m_T(x)$ does not distinguish traps and intermediate states. It could even be possible that the probability to be in a trap is even larger than the probability to be in an intermediate state. To distinguish traps from intermediate states, and different reaction pathways, another stochastic descriptor is needed. This descriptor should tell where the flux of reactive pathways is larger. For example, for a trap region, the flux across its boundary is zero. This quantity is a vector field $J_T(x)$, called transition path current, defined on $\Omega \setminus (R \cup P)$ which is such that, given any region C in that domain, its surface integral across ∂C is equal to the probability flux of reactive trajectories across ∂C. By ergodicity, $J_T(x)$ is defined by imposing the following identity, that must hold true for any $C \subset \Omega \setminus (R \cup P)$:

$$\begin{aligned}\lim_{s\to 0^+} \frac{1}{s} \lim_{T\to\infty} \int_{-T}^{T} (\mathbb{1}_C(x(t))\mathbb{1}_{\Omega\setminus C}(x(t+s)) - \mathbb{1}_{\Omega\setminus C}(x(t))\mathbb{1}_C(x(t+s)))\times \\ \times \mathbb{1}_R(x(t^-_{RP}(t)))\mathbb{1}_P(x(t^+_{RP}(t+s)))dt = \int_{\partial C} J_T(x)\cdot d\sigma_C\end{aligned} \tag{15}$$

This equality represents the rate of how many reactive trajectories go in and out the region C. $J_T(x)$, just as $m_T(x)$, admits a representation in term of committor function. The derivation is a

bit more involved respect to the case of the transition path density, therefore the reader is refereed to the references for a proof. The final expression in the case of Langevin overdamped dynamics is:

$$J_T(x) = D\nabla q(x)\frac{e^{-\beta V(x)}}{\mathcal{Z}} \tag{16}$$

The diffusion constant $D = k_B T/\gamma$ fixes the time scale. The gradient of the committor functions gives information about the direction of the reaction in configuration space.
By virtue of the backward Kolmogorov equation (10), the transition path current results to be a divergence-free vector field, consistent with the fact that the total probability flux of reactive trajectories across any closed surface in $\Omega \setminus (R \cup P)$ must be zero. On the other hand, the flux across any dividing surface S, *i.e.* a surface that entirely separates reactant and product, is non zero and equal by definition to the reaction rate:

$$k = \int_S J_T(x) \cdot d\sigma_S \tag{17}$$

As shown in [MSVE06], this surface integral can be rewritten as the following volume integral:

$$k = D\int_{\Omega\setminus(R\cup P)} |\nabla q(x)|^2 \frac{e^{-\beta V(x)}}{\mathcal{Z}} dx \tag{18}$$

This is quite interesting, because if we look this integral as a functional of the committor, the associated Euler-Lagrange equation gives exactly the Backward-Kolmogorov equation (10), thus allowing to regard the committor function as the solution of a variational problem.
The committor function $q(x)$ provide a useful foliation of the configuration space given by the iso-committor surfaces, *i.e.* the sub-manifolds defined by the constrain $q(x) = c \in [0, 1]$. These are the only sub-manifolds of co-dimension 1 which have the property that the probability distribution that a reactive trajectory pass through them at some point x coincides with the equilibrium probability distribution restricted to these surfaces. Indeed, for x such that $q(x) = c$, $m_T(x) \propto m(x)$. The committor function is a function in configuration space that clearly distinguish reactant from product and which is monotonically increasing from the former to the latter ($0 = q(x)\big|_{x\in R} \neq q(x)\big|_{x\in P} = 1$). It is the slowest variable in the system, since all the *d.o.f.* orthogonal to $\nabla q(x)$ (*i.e.* those on the iso-committor surfaces) are instantaneously thermalized. The value of the committor function is therefore the ideal reaction coordinate. This special property of the committor function can also be used to define the so called transition tubes in configuration space, which are tubes inside which the reactive trajectories stay confined with a fixed probability. Let Σ_c be the iso-committor surface where $q(x) = c$, and $A_c \subset \Sigma_c$ such that:

$$\int_{A_c} J_T(x) \cdot d\sigma = c\int_{\Sigma_c} J_T(x) \cdot d\sigma \tag{19}$$

The surface A_c identify a so called $c-$transition tube, *i.e.* a tube inside which reactive trajectories stay confined with probability c. This tube is generated from the surface A_c by evolving each point in A_c with the artificial dynamics:

$$\frac{dx^i(\tau)}{d\tau} = J_T^i(x(\tau)) \tag{20}$$

where τ is the parameter of the streamlines of the current, without direct physical interpretation. By solving this artificial dynamics backward until ∂R and forward up to ∂P, the $c-$transition tube is identified. If it happens that a rather localized tube is found carrying a large percentage of reactive trajectories, this means that a main reaction channel has been identified. Similarly, a disconnected transition tube is an indicator of the presence of multiple reaction channels.
Finally, since the probability density on the iso-committor surfaces is simply the equilibrium probability density, it is easier to sample these surfaces, as equilibrium techniques can be exploited. The difficult part of TPT is to solve the Backward-Kolmogorov equation (10), being a PDE for a function of several variables, especially for systems with a large number of *d.o.f.*, such as macromolecules, that are some of the interesting systems to which TPT can be usefully applied. To tackle this problem, several techniques and algorithm were developed, and many of them are still a current research topic. To cite an example, the string method is such an algorithm ([ERVE02]). The explanation of these techniques is beyond the scope of this project, so the reader is refereed to the references for details.

4 Numerical implementation of TPT to simple systems

4.1 Link to GitHub repository for the code

The code is available in the linked GitHub repository:
https://github.com/vincenzozimb/TransitionPathTheory.git

4.2 Introduction and numerical aspects

The aim of this section is to apply TPT to a couple of simple two dimensional systems, for which the backward Kolmogorov equation (10) can be numerically solved. In this way, the transition path density and the transition path current can be calculated, and the mechanism of the reaction can be inferred, showing the appropriateness of TPT to the understanding of rare events.
The code was written in the Python language, and the computational expensive part is the numerical solution of the backward Kolmogorov equation, for which an iterative scheme based on the finite difference method was implemented. Central difference expressions were used for approximating both first and second derivatives, while forward and backward differences were appropriately used to deal with Neumann boundary conditions. Specifically, null-normal derivative was imposed at the boundary of the simulation box, meaning imposing no flux of reactive trajectories across it. As an initial guess, the committor function was initialized to the mid-value of $q_{ij}^{(0)} = 0.5$ everywhere in the simulation domain, except in the regions defining the reactant and the product states, in which the Dirichlet boundary conditions (11) were imposed. At every iteration, the value of the committor in each grid point was updated according to the expression obtained from the finite difference approximation and the values of the committor at the previous iteration. More precisely, applying the finite difference discretization scheme to (10) and re-arranging with a little algebra, it is possible to get the functional relation $q_{ij}^{(k+1)} = q_{ij}^{(k+1)}(q_{i\pm1,j\pm1}^{(k)})$ between the committor at every grid point at step $k+1$ and the committor at step k and at grid points compatible with the second order nature of the PDE being solved.
The expressions of the two potential energy functions, and the numerical value of some parameters, are taken from [MSVE06]. However, the discretization step and the number of iterations in the PDE-solver were chosen in order to balance stability of the solution and computational time. For this reason, the results are able to grasp the mechanism of the reactions, but they are not accurate enough to correctly calculate the reaction rate, which in fact is not shown in the results. The aim of this project is to provide a code which is intended to run quickly in portable laptops, and which is able to provide an intuitive explanation of TPT, rather than obtaining accurate numerical results for a toy model. More precisely, in order to run a similar simulation to that in the previously cited paper, finer grids should be used, which in turn imply a large number of necessary iterations in order to reach convergence, considerably increasing the time required to run each simulation.
Each of the simulated system is simple enough to have an intuitive picture of what the mechanism of the reaction should be (which is explained in each section), and then it will be shown how TPT confirms the expected behaviours. In every example the friction coefficients are chosen to be one along each spatial dimension, leaving only the inverse temperature β as a free parameter.

4.3 Symmetric double well

The first reaction to be studied is the diffusion in a symmetric double well potential of the form:

$$V(x,y) = \frac{5}{2}(x^2-1)^2 + 5y^2 \tag{21}$$

which is a combination of a double well potential along the $x-$axis and an harmonic potential along the $y-$axis. For this system, the simulation box is chosen to be $\Omega = [-1.5, 1.5] \times [-1, 1]$, as the potential is large enough at its boundary. The inverse temperature is chosen to be $\beta = 1$, and the meta-stable states (reactant and product) are identified by the condition $V(x,y) < V_{max} = 0.4$. A contour plot of the potential, together to the associated Gibbs distribution $m(x) = e^{-\beta V(x,y)}/\mathcal{Z}$, is plotted in figure 1.

The rare transition consists in going from the low-energy state on the left to the one on the right by pure diffusion. Due to the presence of the energy barrier the system is likely found on one of the two states, and the transition is a rare event. Indeed, this can be noted from any long trajectory generated by solving the over-damped Langevin equation (2) according to the scheme (5), see figure 2. As it is possible to see, the system spends most of the time in the meta-stable

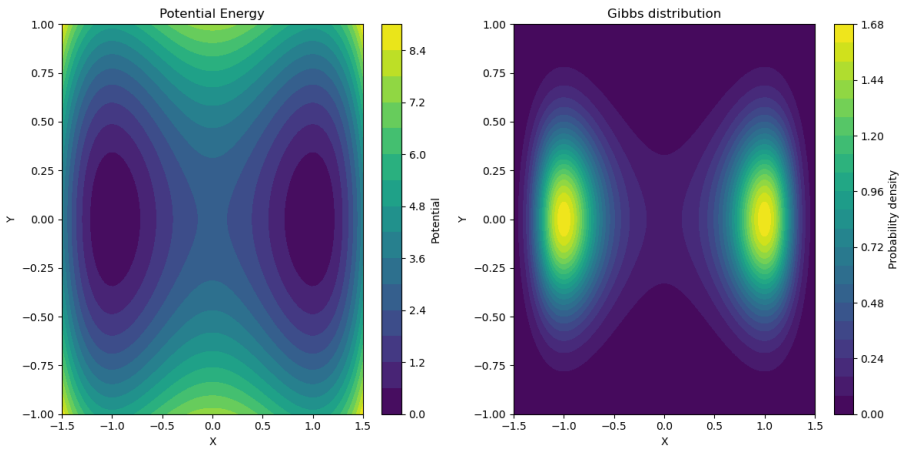

Figure 1: Contour plot of the potential and of the Gibbs distribution for the symmetric double well potential, results for $\beta = 1$.

states, and even if the trajectory is very long, only a couple of transitions occurred. This example shows clearly why standard simulation approaches, such as molecular dynamics, are not able to catch the reaction mechanism. In order to use a trajectory of this kind to study the reaction, one should "prune" it, obtaining only the reactive pieces, and a very long trajectory is needed for obtain a statistical significant sample. Despite this could be achieved for this simple system (indeed in [MSVE06] the authors compare TPT and MD results), it is in general a not feasible approach, as it requires longer and longer trajectories as the dimensionality and complexity of configuration space increases, or simply as the temperature decreases, making the simulation of rare events with plain molecular dynamics is practically impossible. Moreover, for more complicated SDE's, the simple Euler-Maruyama integration scheme (5) becomes unstable, thus more sophisticated and computationally expensive algorithm would be required.

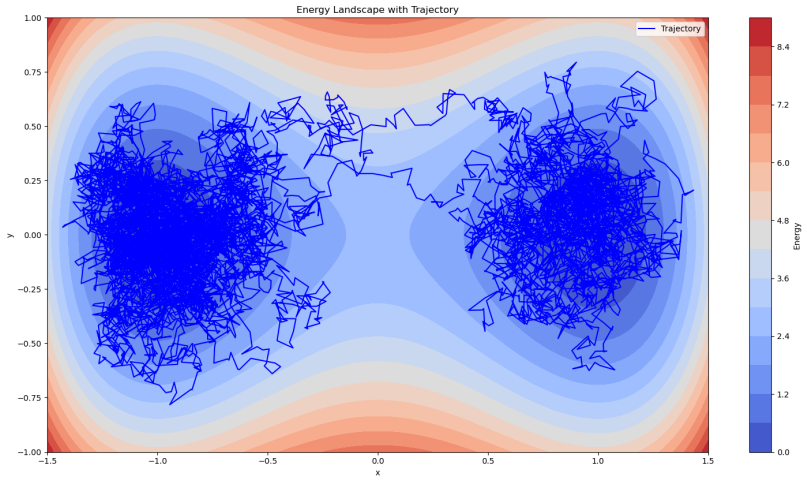

Figure 2: A realization of a long trajectory generated from the over-damped Langevin dynamics. Only a couple of transitions occur in this specific realization.

Let us now move on Transition Path Theory. Given the symmetric shape of the energy landscape, and the symmetry between reactant and product, we expect the iso-committor surfaces to also reflect this symmetry, and the line $\{(x, y) \in \Omega : x = 0, -1 < y < 1\}$ to be the 0.5 iso-committor surface. This prediction is confirmed by the numerics, indeed the numerical solution of the backward Kolmogorov equation provides the committor function depicted in figure 3, together with the kernel of the corresponding transition path density $m_T(x, y) \propto m(x)q(x)(1 - q(x))$.
From the plot of the transition path density we infer that most of the reactive trajectories pass through the local maximum of the potential, located at the center of the configuration space, as

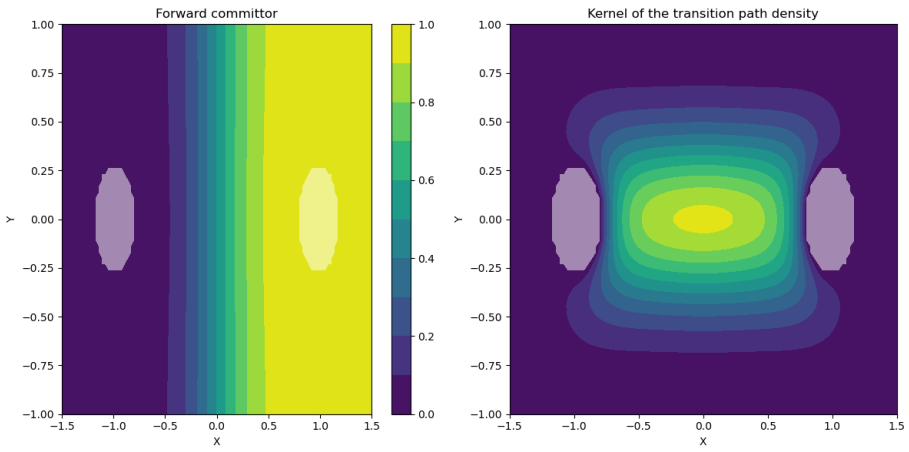

Figure 3: Committor function and kernel of the transition path density. The highlighted regions correspond to the reactant and product states on the left and right, respectively.

expected from symmetry considerations. For this particular highly-symmetric system, the knowledge of the transition path density is sufficient to infer that any reaction tube is centered at $y = 0$, indeed this in confirmed by the quiver plot of the transition path current, see figure 4.

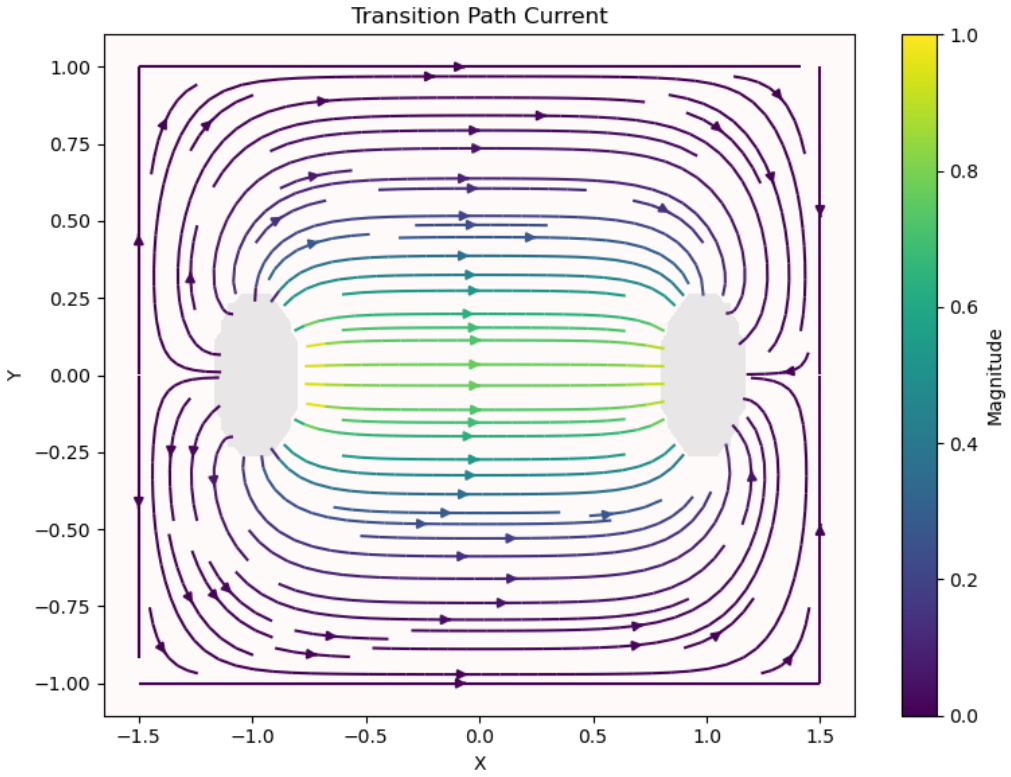

Figure 4: Transition path current between reactant and product states (the highlighted regions). The vector field is re-scaled in such a way to have maximum norm equal to 1.

Observe how there is no flux across $\partial\Omega$, reflecting the Neumann boundary condition $\partial_n q(x)|_{\partial\Omega} = 0$ imposed in solving the backward Kolmogorov equation.

4.4 Triple well potential: entropic switching of the reaction channel

The second system to be studied is interesting because it allows the existence of two different reaction channels, the main one of which is determined by the value of temperature.
The potential energy has the following analytical form:

$$\begin{aligned} V(x,y) =& 3e^{-x^2-(y-1/3)^2} - 3e^{-x^2-(y-5/3)^2} - 5e^{-(x-1)^2-y^2} \\ & - 5e^{-(x+1)^2-y^2} + 0.2x^4 + 0.2\left(y-\frac{1}{3}\right)^4 \end{aligned} \tag{22}$$

The energy landscape is plotted in figure 5.

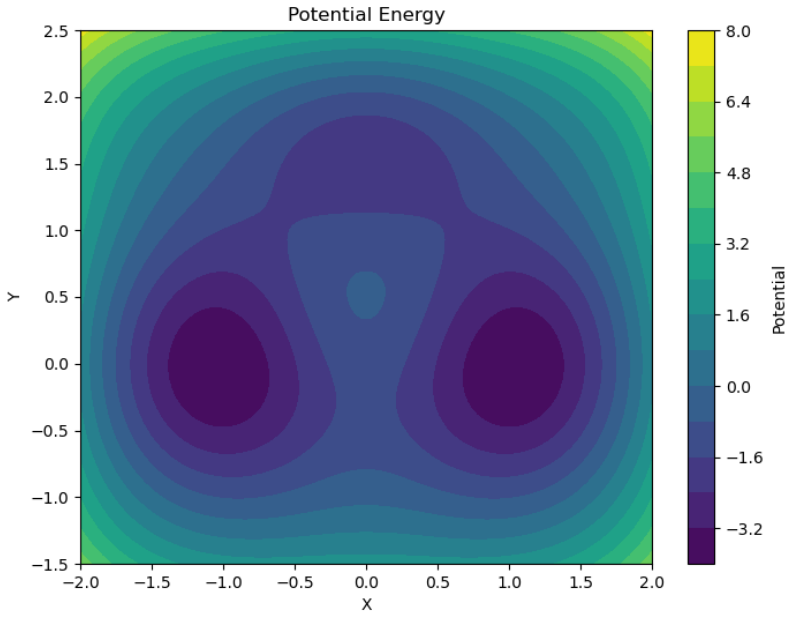

Figure 5: Contour plot of the energy landscape for the three well potential.

There are two deep minima located near $(\pm 1, 0)$ and another local minima around $(0, 1.5)$, while there is a maximum at position $(0, 0.5)$. Among these critical points are three saddle points. As it is possible to infer from the plot, the two deep minima are weakly connected by an indirect path passing through the local minimum at the top, just like a shallow valley. Instead, a direct "minimum length" connection between the two meta-stable states is hindered by the presence of an energy barrier. For this system, the configuration space is chosen to be $\Omega = [-2, 2] \times [-1.5, 2.5]$ and the meta-stable states (reactant and product) are identified by the condition $V(x, y) < V_{max} = -2.5$. The reaction will be studied at two different value of temperature: $\beta_{high} = 1.67$ and $\beta_{low} = 6.67$. In figure 6a and 6b the plots of the Gibbs distributions for the two temperatures are presented.

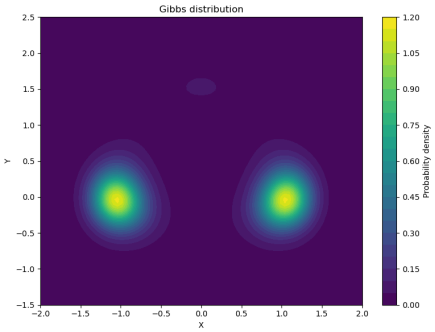

(a) Gibbs distribution for the three-hole potential at β_{high}.

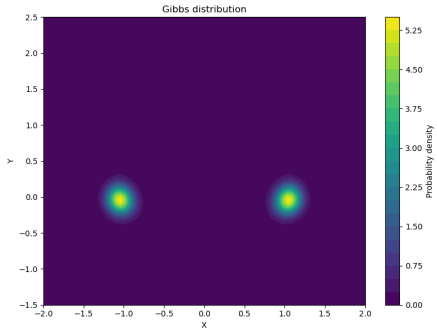

(b) Gibbs distribution for the three-hole potential at β_{low}.

For every fixed y, the potential is symmetric under the exchange $x \leftrightarrow -x$: we expect this symmetry to be preserved in the shape of the iso-committor surfaces and correspondingly also for the transition path density. This is confirmed by the numerics (within the numerical approximation errors), as shown in figure 7 for the high temperature case

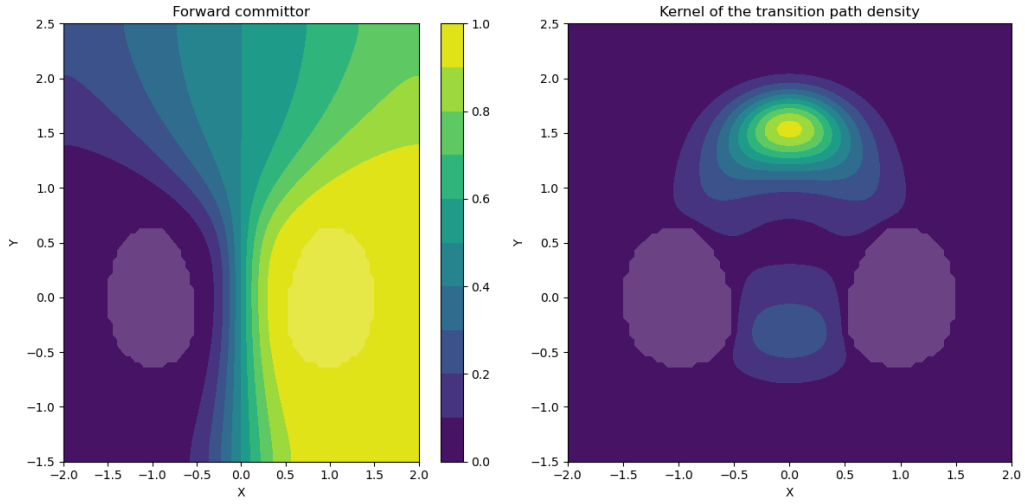

Figure 7: Iso-committor surfaces and transition path density for the three-hole potential in the β_{high} case. The highlighted regions represent the meta-stable states.

and in figure 8 for the low temperature case

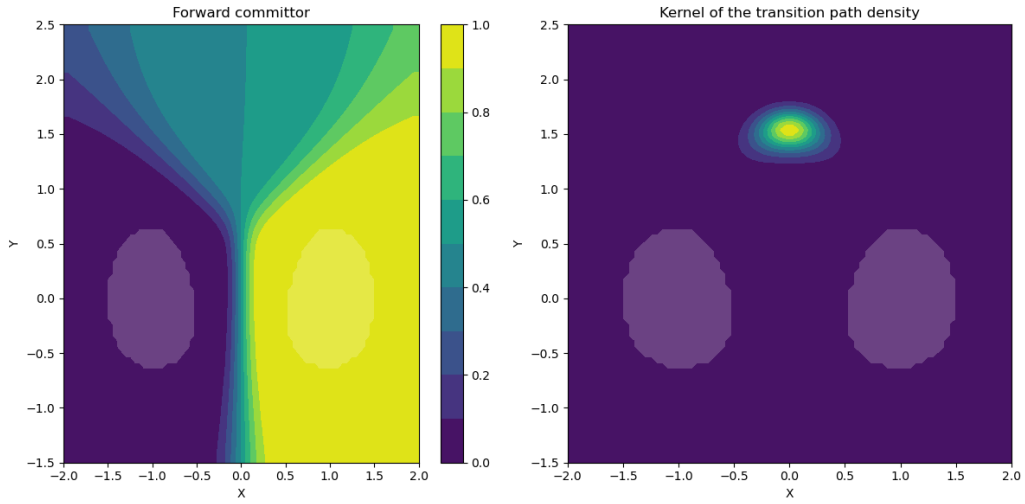

Figure 8: Iso-committor surfaces and transition path density for the three-hole potential in the β_{low} case. The highlighted regions represent the meta-stable states.

For this system, the transition path density allow to infer that in the high temperature case a second reaction channel is opened, but in order to fully understand the interplay between the two reaction channels the transition path current is a necessary quantity. At low temperature, the thermal fluctuations are not strong enough to overcome the energy barrier, thus we expect the reaction to proceed along the upper channel, following the aforementioned valley. However, increasing the temperature, entropic effects become more important, and as a consequence the system becomes able to overcome the barrier, arriving to the product state also following the more direct, "minimum length" path. This mechanism is clearly visible in the behaviour of the transition path current, see figures 9a and 9b. Also in this case, the vector field is re-scaled in such a way that the maximum of its norm is one.

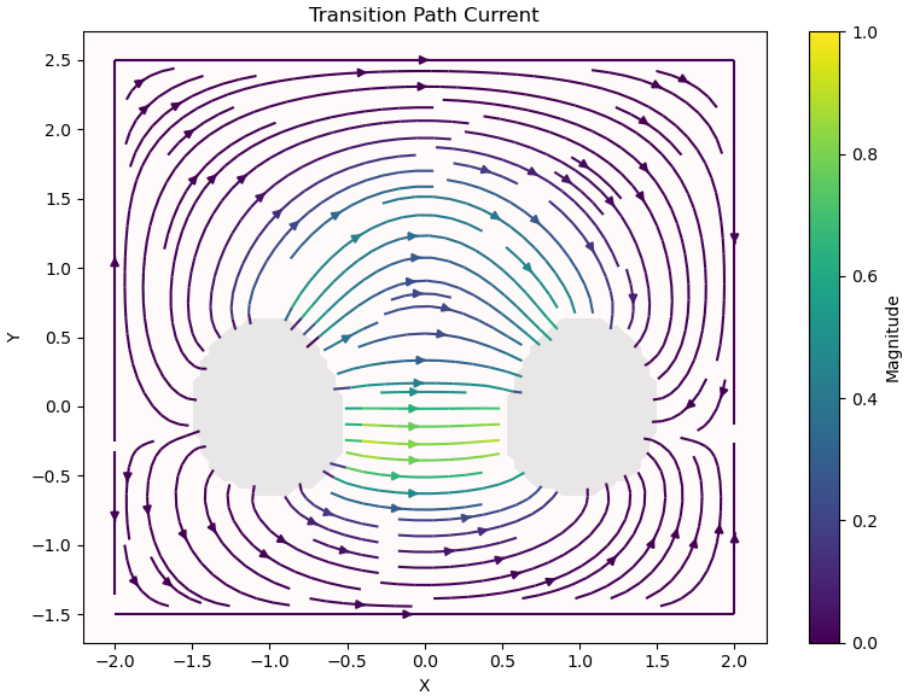

(a) Quiver plot of the transition path current at β_{high}. The highlighted regions represent the meta-stable states.

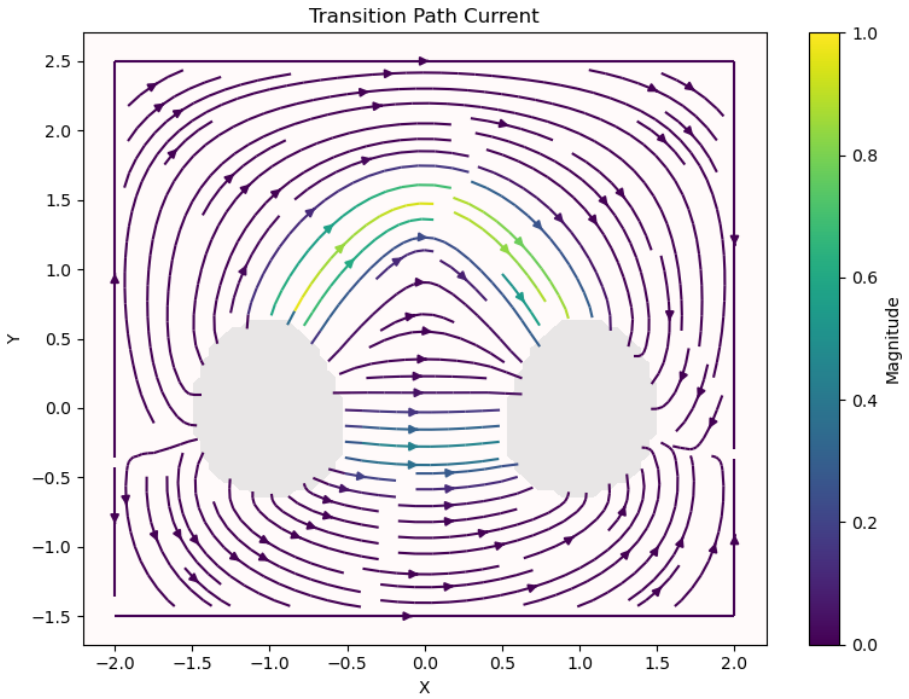

(b) Quiver plot of the transition path current at β_{low}. The highlighted regions represent the meta-stable states.

This example shows how Transition Path Theory is also able to take into account both energetic and entropic effects, and that quantities such as temperature are simply parameters whose value does not increase or decrease the complexity of the computation (which is the case for direct plain molecular dynamics simulation).

A Proof that $q(x)$ satisfies the bK equation from stochastic dynamics using path integral formalism

The aim of this appendix is to justify the validity of (10). There are several way to prove this statement, here the derivation using the path integral formalism will be followed. Before proving this however, a brief recap of the main concepts and quantities in stochastic dynamics is needed. Not all the proofs will be provided here, and the reader is refereed to any book on the physical theory of stochastic dynamics for the derivations and for more details.
The evolution of any system whose dynamics involve a stochastic behaviour is governed by a specific SDE; for instance a physical system whose dynamics is described, at least in some regime, by (2) is said to obey the over-damped Langevin dynamics. By solving several times the SDE, one is allowed, at least conceptually, to calculate the empirical probability distribution to find the system at a particular position of its configuration space at a particular time. This probability distribution will satisfy a particular partial differential equation, which is called the Fokker-Planck (FP) equation associated to the stochastic process. In the case of the over-damped Langevin dynamics, the associated FP equation is the so called *Smoluchowski-Fokker-Planck* equation:

$$\frac{\partial P(x,t)}{\partial t} = D[\nabla^2 + \beta(\nabla^2 V(x) + \nabla V \cdot \nabla)]P(x,t) \tag{23}$$

Defining $\hat{H}_{FP} = -D[\nabla^2 + \beta(\nabla^2 V(x) + \nabla V \cdot \nabla)]$ equation (23) assumes the form of a Schrodinger equation in imaginary time: $\partial_t P = -\hat{H}_{FP} P$. This allows, in analogy to the quantum mechanical case, to provide a path integral representation for the propagator $p(x,t|x_0,t_0)$, which turns out to be:

$$p(x,t|x_0,t_0) = \mathcal{N} e^{-\frac{V(x)-V(x_0)}{2k_B T}} \int_{x_0}^{x} \mathcal{D}q \exp\left(-\int_{t_0}^{t} d\tau \frac{\dot{q}(\tau)^2}{4D} + V_{\text{eff}}(q(\tau))\right) \tag{24}$$

$$V_{\text{eff}}(x) = \frac{D}{4(k_B T)^2}\left[|\nabla V(x)|^2 - 2k_B T \nabla^2 V(x)\right] \tag{25}$$

The exponential prefactor in front of the path integral is not present in the quantum mechanical case: it takes into account the fact that $\hat{H}_{FP}$ is not an hermitian operator respect to the standard L^2 scalar product. Therefore the Smoluchowski-Fokker-Planck and its adjoint equation are two different equations. In particular, $\hat{H}^{\dagger}_{FP} := \hat{H}_b = D(\nabla^2 - \beta \nabla V \cdot \nabla)$, and the corresponding stationary equation is the backward Kolmogorov equation (10). Moreover, applying time reversal arguments, it turns out that if $p(x,t|x',t')$ solves the equation for $\hat{H}_{FP}$, then it also solves the equation (up to a sign) for $\hat{H}'_b$, so respect to the initial conditions (for this reason it is called the *backward* equation).
The interpretation of $p(x,t|x_0,t_0)$ is as the probability for the system to be found at position x at time t given the initial condition x_0 at time t_0. This allow to derive a path integral representation for the probability to go from x_0 to x in a time t, without ever touching the boundary of a specific domain W. This probability, say $P^*_W(x,t|x_0)$, is given by the same path integral of (24), adding to $V_{\text{eff}}(x)$ the additional term $\Omega_W(x)$, which is zero outside W and diverge inside and at the boundary of W, suppressing all paths through this domain. This implies that $P^*_W(x,t|x_0) \neq 0$ only for $x \notin W$. This condition can be imposed in the equation $P^*_W(x,t|x_0)\Omega_W(x) = 0$, which in turn implies that $P^*_W(x,t|x_0)$ also satisfy the Smoluchowski-Fokker-Planck equation (23).
The **survival probability** $S_W(t|x_0)$ is the probability of not having entered in W at time t, given initial condition x_0. It is given by:

$$S_W(t|x_0) = \int_{W^c} dx P^*_W(x,t|x_0) \tag{26}$$

It follows that $1 - S_W(t|x_0)$ is the probability of having entered in W before time t, starting from some x_0 from the outside. This probability is linked to the **first passage time distribution** $F_W(t|x_0)$, which represent the probability of crossing ∂W for the first time exactly at time t, by the following relation:

$$\int_0^t dt' F_W(t|x_0) = 1 - S_W(t|x_0) \tag{27}$$

Thus:

$$
\begin{aligned}
F_W(t|x_0) &= -\frac{\partial}{\partial t} S_W(t|x_0) \\
&= -\frac{\partial}{\partial t} \int_{W^c} dx P^*_W(x,t|x_0) \\
&= -D \int_{W^c} dx \nabla \cdot (\nabla + \beta \nabla V(x)) P^*_W(x,t|x_0) \\
&= + \int_{\partial W} d\vec{\sigma} \cdot D \left(\nabla P^*_W(x,t|x_0) + \beta \nabla V(x) P^*_W(x,t|x_0) \right) \\
&:= \int_{\partial W} d\vec{\sigma} \cdot \vec{J}^*_W(x,t|x_0)
\end{aligned}
\tag{28}
$$

So the first passage time distribution can be viewed as the flux of the vector current $\vec{J}^*_W(x,t|x_0)$. If $W = R \cup P$ (reactant and product), the flux of $\vec{J}^*_W(x,t|x_0)$ across ∂P, integrated over time, gives by definition exactly the forward committor function:

$$
q(x) = \int_0^\infty dt \int_{\partial P} d\vec{\sigma}' \cdot \vec{J}^*_W(x',t|x) = D \int_0^\infty dt \int_{\partial P} d\vec{\sigma}' \cdot (\nabla' + \beta \nabla V(x')) P^*_W(x',t|x) \tag{29}
$$

Now, recalling that if $P^*_W(x',t|x)$ satisfy (23) then it also satisfies the backward equation respect to the initial conditions:

$$
\frac{\partial P^*_W(x',t|x)}{\partial t} = + \hat{H}_b P^*_W(x',t|x) \tag{30}
$$

Thus, applying the $\hat{H}_b$ operator on both sides of (29):

$$
\begin{aligned}
\hat{H}_b q(x) &= D \int_0^\infty dt \int_{\partial P} d\vec{\sigma}' \cdot (\nabla' + \beta \nabla V(x')) \hat{H}_b P^*_W(x',t|x) \\
&= D \int_0^\infty dt \int_{\partial P} d\vec{\sigma}' \cdot (\nabla' + \beta \nabla V(x')) \frac{\partial}{\partial t} P^*_W(x',t|x) \\
&= \int_0^\infty dt \frac{\partial}{\partial t} \int_{\partial P} d\vec{\sigma}' \cdot D (\nabla' + \beta \nabla V(x')) P^*_W(x',t|x) \\
&= \int_0^\infty dt \frac{\partial}{\partial t} F_P(t|x) \\
&= F_P(\infty|x) - F_P(0|x) = 0 - 0 = 0
\end{aligned}
\tag{31}
$$

The last step in the derivation holds because at time zero the system is outside P with probability one, and for $t \to \infty$ the first passage time distribution goes to zero by ergodicity.
Therefore the thesis is proved, that is:

$$
\boxed{(\nabla^2 - \beta \nabla V \cdot \nabla) q(x) = 0} \tag{32}
$$

Bibliography

[BOF18] G. Bartolucci, S. Orioli, and P. Faccioli. Transition path theory from biased simulations. *The Journal of Chemical Physics*, 149(7):072336, aug 2018.

[ERVE02] Weinan E, Weiqing Ren, and Eric Vanden-Eijnden. String method for the study of rare events. *Phys. Rev. B*, 66:052301, Aug 2002.

[ERVE05] Weinan E, Weiqing Ren, and Eric Vanden-Eijnden. Transition pathways in complex systems: Reaction coordinates, isocommittor surfaces, and transition tubes. *Chemical Physics Letters*, 413(1):242–247, 2005.

[EVE10] Weinan E and Eric Vanden-Eijnden. Transition-path theory and path-finding algorithms for the study of rare events. *Annual Review of Physical Chemistry*, 61(1):391–420, 2010. PMID: 18999998.

[FCBVE06] Mauro Ferrario, Giovanni Ciccotti, Kurt Binder, and Eric Vanden-Eijnden. *Transition Path Theory*. 01 2006.

[Hum03] Gerhard Hummer. From transition paths to transition states and rate coefficients. *The Journal of Chemical Physics*, 120(2):516–523, 12 2003.

[MSVE06] Philipp Metzner, Christof Schütte, and Eric Vanden-Eijnden. Illustration of transition path theory on a collection of simple examples. *The Journal of Chemical Physics*, 125(8):084110, 08 2006.

[SS21] Florian Sammüller and Matthias Schmidt. Adaptive brownian dynamics. *The Journal of Chemical Physics*, 155(13):134107, oct 2021.